Liquid/liquid encapsulation: effects of wettability and miscibility

D. Baumgartner[1], P. Benez[1], G. Brenn[1], and C. Planchette[1*]
[1]Institute of Fluid Mechanics and Heat Transfer, Graz University of Technology, A-8010 Graz, Austria
*Corresponding author: carole.planchette@tugraz.at

Abstract
In-air microfluidics has appeared as a promising liquid/liquid encapsulation method. Yet, to date, only limited studies are available dealing either with miscible liquids or totally wetting immiscible ones and focusing on the regimes produced by the collisions between a drop stream and a jet. In this work, we investigate the effects of liquid wettability and miscibility on the encapsulation of liquid drops by a continuous liquid jet. Drops are made of an aqueous solution of glycerol and combined with three different liquids of comparable surface tension (24 mN/m +/- 4 mN/m) and viscosity (5 mPa.s): silicon oil, n-hexadecane and an aqueous solution of ethanol and glycerol. First, for each system, we systematically probe the limits of the observed regimes and document their possible shifts. The results are then interpreted by carefully following the extension of the drop in terms of surface and kinetics. The maximal drop surface extension is well predicted using the drop Weber number, and the kinetics of this extension scales with the drop capillary time scale. This finding calls for a description of the drop fragmentation threshold based on the drop Weber number.

Keywords
drop, jet, encapsulation, fragmentation, wetting, miscibility

Introduction

It has been proposed to use the collisions between pairs and triplets of drops [1, 2], and between drops and a continuous liquid jet [3] to encapsulate drops in spherical liquid shells or in cylindrical continuous jets. This method, also called in-air microfluidics, enables the production of precursors to well defined and controlled spherical capsules and fibres [4, 5]. Yet to date, only a few investigations of drop-jet collisions have been made [4, 6, 7]. Motivated by potential biomedical applications, for which the restrictions on the materials go beyond liquid jettability and drop producibility, this work investigates the effects of liquid wettability and miscibility on the outcome of drop-jet collisions. Restricting our study to head-on collisions, we consider three different pairs of liquids. The liquids: silicon oil, n-hexadecane and an aqueous solution of ethanol and glycerol are selected to have comparable surface tension and viscosity. They are combined with the same aqueous glycerol solution reducing the material properties variations to those of their interfacial tension and providing pairs of immiscible liquids with the jet totally and partially wetting the drops, and a pair of miscible liquids. Our experimental approach consists in systemically probing the collision outcomes for the three liquid pairs scanning a wide range of relative drop-jet velocity and drop spacing. The observed regimes are documented with special emphasis for the *drops-in-jet* regime and its limits to the first occurrence of fragmentation. For each liquid pair, we vary the drop spacing between two extreme values and report for the whole studied range the observed outcomes for increasing inertia using the modified Weber number We^* introduced in [7]. We thus propose possible reasons to explain the shift in the capillary fragmentation threshold. To better describe the inertial fragmentation thresholds and understand the mechanisms at stake, we closely observe the evolution of the drops during the collisions. The expansion (surface and kinetics) of dyed drops is recorded using two cameras providing orthogonal views. In the light of these results, the relevance of We^* is compared to the one of We_d, the drop Weber number.
The liquids and their properties as well as the experimental set-up are presented in the section **Materials and methods**. In the **Results and discussion** section, the regime maps are shown together with our results regarding the drop expansion. This article finishes with the conclusions.

Materials and methods

In this paper, the subscript j is used to designate the jet or the jet liquid, d the drops or the drop liquid, and dj the interface between them. The experimental methods being already described in detail elsewhere [3, 7], only the main features are recalled here.

Liquids

The liquids are selected to obtain similar viscosity μ. Furthermore, the jet liquids have comparable surface tension σ_j so that the three liquid pairs differ mainly by their interfacial tension σ_{dj}. Combining drops of an aqueous glycerol solution at 50% in weight (G5) with a jet of silicon oil (SO5) provides immiscible liquids with total wetting of the jet. Indeed, the spreading parameter S defined as $S = \sigma_d - \sigma_j - \sigma_{dj}$ is strictly positive, equal to $13\ mN \cdot m^{-1}$ [8, 9]. Replacing SO5 by hexadecane (hexa) gives immiscible liquids with partial wetting as reported for hexadecane/water for which $S \approx -8mN/m$, [10, 11]. Finally, by using a mixture of ethanol and glycerol in water (EtOH), we obtain a jet totally miscible with the drops. The interfacial tension is thus taken equal to 0.

For completeness the liquid properties are listed in Table 1.

Table 1. Liquid properties of the selected liquids. The values are obtained at $22 \pm 2\ ^oC$, $*$ indicates values from the literature on similar systems, [8, 9, 10, 11].

used for	abbreviation	$\rho\ [kg \cdot m^{-3}]$	$\mu\ [mPa \cdot s]$	$\sigma\ [mN \cdot m^{-1}]$	$\sigma_{dj}\ [mN \cdot m^{-1}]$
Drops	G5	1120 ± 10	4.97 ± 0.05	67.5 ± 2	- -
Jet	SO5	915 ± 10	5.10 ± 0.05	19.5 ± 0.5	$35.0^* \pm 3$
Jet	Hexa	767 ± 10	3.50 ± 0.30	25.5 ± 0.5	$50.0^* \pm 4$
Jet	EtOH	936 ± 10	4.58 ± 0.4	25.7 ± 0.7	0

Set-up and problem parameters

The experimental set-up is made of a droplet generator producing a stream of drops (dyed, diameter $D_d = 200 \pm 20\ \mu m$) and a nozzle providing a jet of a different liquid (not dyed, diameter $D_j = 300 \pm 10\ \mu m$). The flow rates are set by two independent pressurized tanks. The trajectories of the drops and jet are finely adjusted using micro-traverses to obtain head-on collision (no eccentricity). The collisions are recorded using a stroboscopic illumination at the frequency of the drop production and two cameras providing side and front views, see Fig. 1a). Furthermore, special care is given to adjust the relative velocity of the jet and drops $\vec{U}$ in order to cancel its tangential component $U_{\parallel}$; leaving $U \approx U_{\perp}$, see Fig. 1b).

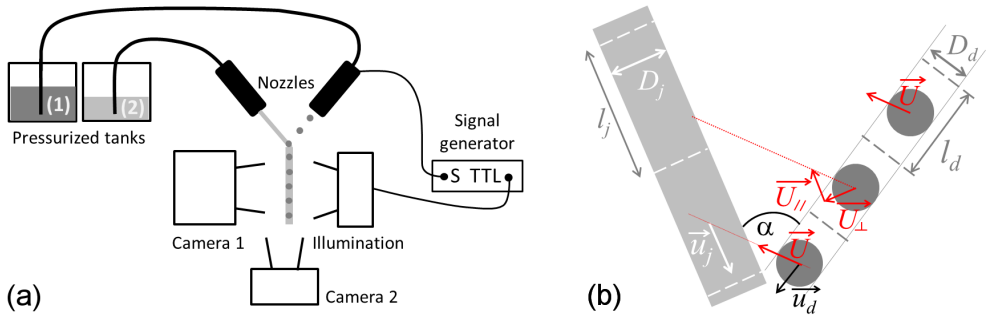

Figure 1. (a) Sketch of the experimental set-up including 2 cameras for systematically recording the front and side views of the collisions. (b) Sketch of a collision defining the relevant parameters. In this article only the collisions with $U_{\parallel} = 0$ are investigated.

Results and discussion

Regimes

For clarity, the regimes have been illustrated using the simple sketches of Fig. 2 where the jet liquid is white, the drop liquid black and, if miscible, a mixture of them is gray. Illustrative pictures with the drops moving from the left to the right are also shown in Figs. 3 and 4.

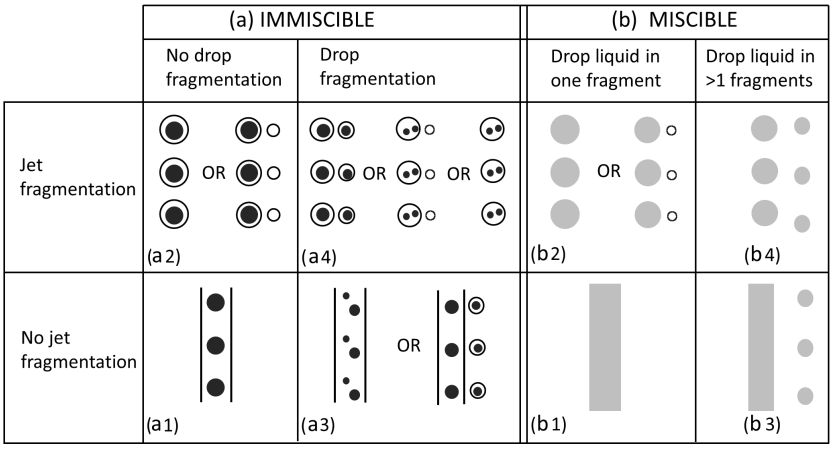

Figure 2. Regimes for (a) immiscible liquids: (1) *drops-in-jet*, (2) *encapsulated drops*, (3) *fragmented drops in jet*, (4) *mixed fragmentation*; and (b) miscible liquids: (1) *drops-in-jet*, (2) *fragmented jet*, (3) *fragmented drops in jet*, (4) *mixed fragmentation* .

For immiscible liquids, four main regimes can be defined [3, 7].

- *Drops-in-jet* takes place when the drops are regularly embedded in the jet without fragmenting or fragmenting the jet. See Figs. 2 (a1) and 3 (a1).
- *Fragmented drops in jet* is found when the drops fragment, but not the jet. Often, all drop fragments remain inside the continuous jet where they are encapsulated. Sometimes, some of the drop fragments are expelled from the jet dragging a small portion of the jet which, nevertheless, stays continuous. See Figs. 2 (a3) and 3 (a3).
- *Encapsulated drops* which results from the fragmentation of the jet, the drops remaining not fragmented. The jet fragmentation can take place with or without satellites. See Figs. 2 (a2) and 3 (a2).
- *Mixed fragmentation* which corresponds to the fragmentation of both the drops and the jet. See Figs. 2 (a4) and 3 (a4).

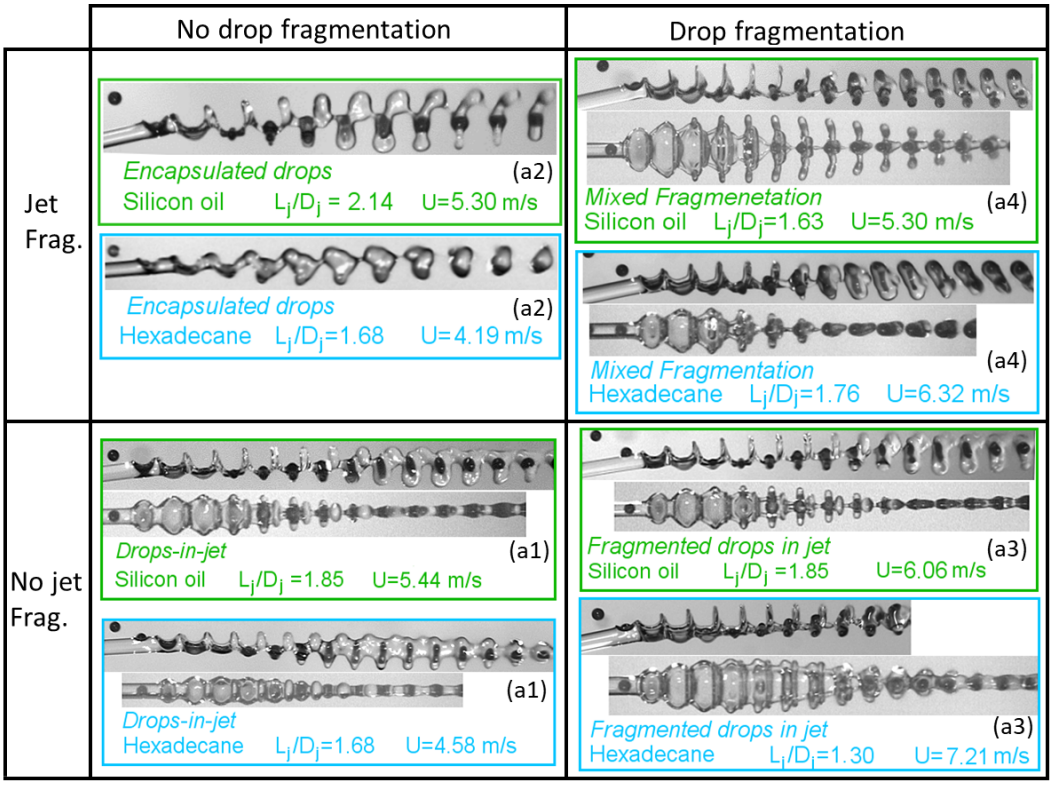

Figure 3. Pictures illustrating the regimes sketched in Fig. 2a) for immiscible liquids. Jet of silicon oil: green boxes; and jet of hexadecane: blue boxes. Two pictures shown in the same box correspond to two views of the same collision.

For miscible liquids, since no interface exists between the drop liquid and the jet liquid, the regimes must be re-defined. Indeed, one cannot consider drop fragmentation except the drop liquid is found in separated fragments. Thus, the re-definition of the regimes is based on the distribution of both liquids after collision. Practically, the fragment composition is determined by colorimetric observation. More precisely, we obtain 4 regimes.

- *Drops-in-jet* is unchanged and consists of merged drops and jet. After the jet has recovered its cylindrical shape, the drop liquid appears to be regularly distributed in the form of a stream of spheres indicating that no significant diffusion occurs during the collision time scale. See Figs. 2 (b1) and 4 (b1).
- *Fragmented drops in jet* is now used to designate collisions leading to a continuous liquid jet accompanied by a stream of satellite drops in which the drop liquid is present. This outcome corresponds for immiscible liquids to fragmented drops in jet where drop fragments are expelled from the jet. Note that fragmented drops in jet with the drop fragments remaining in the jet does not exist with miscible liquids. See Figs. 2 (b3) and 4 (b3)
- *Fragmented jet* corresponds to encapsulated drops for immiscible liquids. The number of fragments containing the drop liquid must be equal to the initial drop number. See Figs. 2 (b2) and 4 (b2).
- *Mixed fragmentation* which corresponds to the fragmentation of the jet and drops. In contrast to immiscible liquids, *mixed fragmentation* cannot be used if the drop liquid is not found in more drops after than before the collision. See Figs. 2 (b4) and 4 (b4).

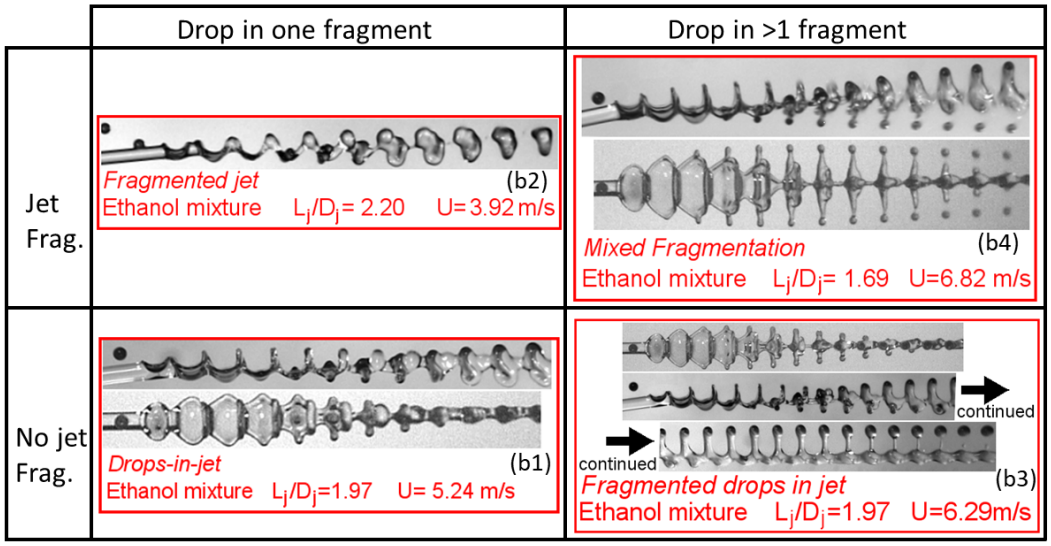

Figure 4. Pictures illustrating the regimes sketched in Fig. 2b) for miscible liquids (jet made of the ethanol mixture: red boxes). Two pictures shown in the same box correspond to two views of the same collision.

Regimes maps

Based on the results obtained with silicon oil and an aqueous solution of glycerol [3, 7], two parameters are used. The first one, L_j/D_j characterizes the collision geometry. It gives the spacing between two consecutive drop impacts normalized by the jet diameter, see Fig. 1b). As already reported, this parameter enables to distinguish *drops-in-jet* and *fragmented drops in jet* found below a critical value from *encapsulated drops* for larger values. In other terms, and even if its critical value - around 2 - is not the same as the classical one found by Rayleigh, L_j/D_j can be used to predict the capillary-driven fragmentation of the jet.

The second parameter $We^* {D_d}^2/D_{dij}L_{dij}$ has been established to compare the maximum extension of the drop to typical distances separating consecutive drops in the *drops in jet* structure. In this context, the maximum diameter of the lamella that forms inside the jet is estimated by scaling based on We^*, a modified Weber number. As proposed in [7], we have:

$$D_{max} \propto D_d We^{*1/2} \qquad We^* = \frac{(\rho_j L_j D_j^2/2 + \rho_d D_d^3/3)U^2}{\sigma_j D_j L_j + \sigma_{dj} D_d^2} \tag{1}$$

It was suggested that to prevent drop fragmentation, the maximal extension of the lamella should not exceed some critical dimensions. These dimensions are on one side D_{dij} the external diameter of the jet after drop encapsulation and L_{dij} to the spacial period of the drops once encapsulated. Indeed if $D_{max} >> D_{dij}$ the drops may fragment inside the jet via, for example, some pinch-off process. The drops may also fragment if $D_{max} >> L_{dij}$. In this case, the drops may first coalesce inside the jet before fragmenting again leaving additional satellites. D_{dij} and L_{dij} are derived from volume and momentum conservation, neglecting viscous losses and assuming a continuous cylinder jet is recovered. This provides:

$$D_{dij} = \tilde{D}_d \frac{(1+m_j/m_d)^{1/2}(1+\rho_d m_j/\rho_j m_d)^{1/2}}{\left[(\cos\alpha + m_j u_j/m_d u_d)^2 + \sin^2\alpha\right]^{1/4}} \qquad \frac{L_{dij}}{L_d} = \frac{\sqrt{(\cos\alpha + m_j u_j/m_d u_d)^2 + \sin^2\alpha}}{1+m_j/m_d} \tag{2}$$

Here, m_j and m_d are the mass of the jet portion or one drop and are given by: $m_j = \pi\rho_j D_j^2 L_j/4$ and $m_d = \pi\rho_d D_d^3/6$. $\tilde{D}_d$ is the equivalent drop stream diameter defined as $\tilde{D}_d^2 = (2/3)(D_d^3/L_d)$, α is the angle between the jet and drop stream axes, see Fig. 1b).

Note that these parameters, initially defined for immiscible liquids, can be used for miscible liquids as well. In this case, σ_{dj} is 0. The results obtained for the three liquid pairs are plotted in Fig. 5. Differences can be observed for the inertial limit with significant shifts of the continuous lines representing the inertial transitions found for different values of $We^* {D_d}^2/L_{dij}D_{dij}$. For the the capillary-driven limit, small variations of the critical L_j/D_j values are observed yet, they remain in the typical range of the experimental uncertainty.

Capillary limit

Changes in the capillary limit could be expected due to the variations of surface and interfacial tensions. Yet, the measured differences are really moderate and remain within the experimental uncertainty. Comparing immiscible liquids only, we observe that the *drops-in-jet* structure may only be slightly stabilized when the jet liquid totally wets the drops. While surface and interfacial tensions are not accounted for by L_j/D_j, purely geometric in nature, the

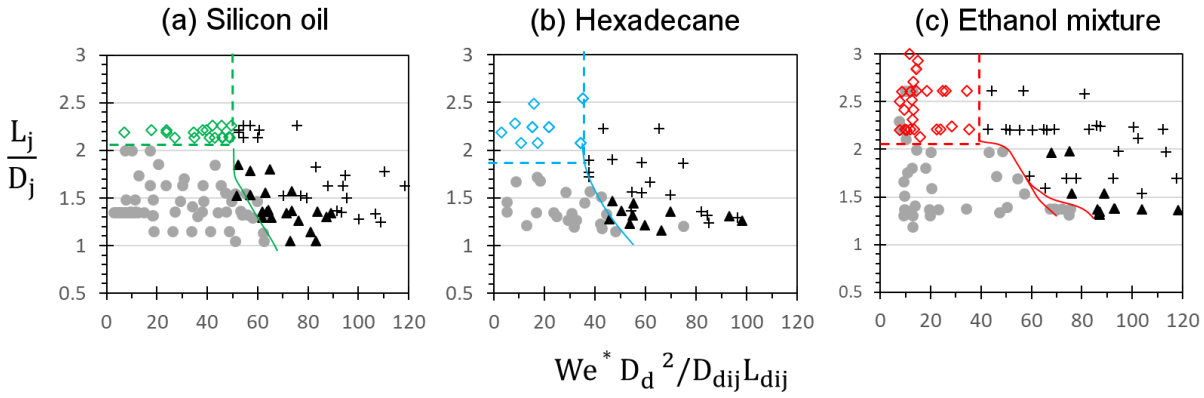

Figure 5. Regime maps obtained using $(L_j/D_j; We^* {D_d}^2/L_{dij}D_{dij})$ [7] for (a) G5/SO5; (b) G5/Hexa; (c) G5/EtOH. Grey circles: *drops in jet*; black triangles: *fragmented drops in jet*; black crosses: *mixed fragmentation*; green and blue diamonds (a-b): *encapsulated drops* and red diamonds (c): *fragmented jet*. The lines are guides for the eye.

presence of the two phases may influence the stability of the *drops-in-jet*. From a thermodynamic point of view, $S > 0$ is expected to favor the engulfment of the drops in the jet and thus to promote the redistribution of the jet liquid in the form of a continuous cylinder. From a mechanical point of view, the smaller the interfacial tension the less important the Laplace pressure of the encapsulated drops. "Softer" drops may generate less important pressure gradients thus lowering the source of the jet instability.
Comparing silicon oil with the ethanol mixture ($S > 0$, immiscible and miscible with the drop liquid, respectively) shows no significant differences except for a few points with low inertia ($We^* {D_d}^2/L_{dij}D_{dij} \approx 10$) where *drops-in-jet* are observed with the ethanol mixture. This phenomenon could be caused by Marangoni flows. Indeed, with ethanol, if the inertia is small enough, one can expect the surface tension to be lower at the "untouched" jet portions than at the impacted points, creating a flow that potentially favors the recovery of a cylindrical shape, thus stabilizing the structure.

Inertial limit

Let us first focus on the immiscible liquids. As shown in Fig. 5 a) and b), changing the wettability of the liquids shifts the inertial fragmentation limit. While for silicon oil the transition is typically found for $We^* {D_d}^2/L_{dij}D_{dij}$ between 50 and 70 for L_j/D_j varying from 1.6 to 1.0, for hexadecane the limit goes from $We^* {D_d}^2/L_{dij}D_{dij}$ close to 35 and up to 55 for similar variations of L_j/D_j. Beside other effects, this difference is likely to be caused by an inaccurate evaluation of D_{max} or by an inappropriate fragmentation criterion, namely $L_{dij}D_{dij}$ as critical dimensions.
We probe these two hypotheses below.
First, we evaluate D_{max} identifying the distorted drop with a bent disk (flat cylinder). Following the notations of Fig. 6, we obtain $D_{max,1} = \pi\,(a+b)\left(1+3\lambda^2/(10+\sqrt{4-3\lambda^2})\right)/2$ with $\lambda = (a-b)\,/\,(a+b)$ from the view 1, and measure $D_{max,2}$ directly from the view 2. We observe no significant differences between these two measures (less than 10% over many collisions) which justifies a priori our choice for the drop shape. We thus use $D_{max} \approx D_{max,1} \approx D_{max,2}$ and plot the normalized surface of the distorted drop Σ_{max}/Σ_d as a function of We^*. Here and as found in the literature [12, 13, 14], Σ_{max} is obtained by identifying the surface of the lamella to the one of a flat cylinder and further assuming drop volume conservation. This provides $\Sigma_{max} = \pi {D_{max}}^2\left(1+2\pi(D_d/D_{max})^3/3\right)$. Classically, we have $\Sigma_d = \pi {D_d}^2$.

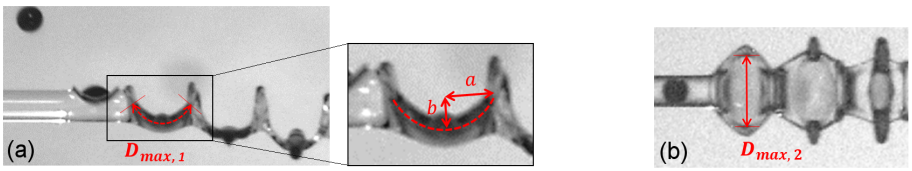

Figure 6. a) View 1 providing $D_{max,1} = \pi\,(a+b)\left(1+3\lambda^2/(10+\sqrt{4-3\lambda^2})\right)/2$ with $\lambda = (a-b)\,/\,(a+b)$ with a and b defined on the picture (Ramanujan approximation). b) View 2 with the definition of $D_{max,2}$.

While for each jet liquid, a linear trend is observed, a discrepancy appears between the data sets obtained with different jet liquids, see Fig. 7a). Plotting the same data against the drop Weber number $We_d = \rho_d D_d U^2/\sigma_d$ provides a very good agreement, see Fig. 7b). Thus, to compare different liquid pairs, it appears that the evaluation of D_{max} should not be done using We^*, as initially proposed in [7] but rather based on We_d.
To confirm this finding, we also investigate the kinetics of the drop extension. We therefore measure T_{max}, the time period required for the drop to reach its maximal extension (counted from the instant of impact). T_{max} normalized by $\tau_{\sigma,d} \propto \sqrt{m_d/\sigma_d}$ is reported in Fig. 7c) as a function of We_d. It can be seen that T_{max} scales with the oscillation

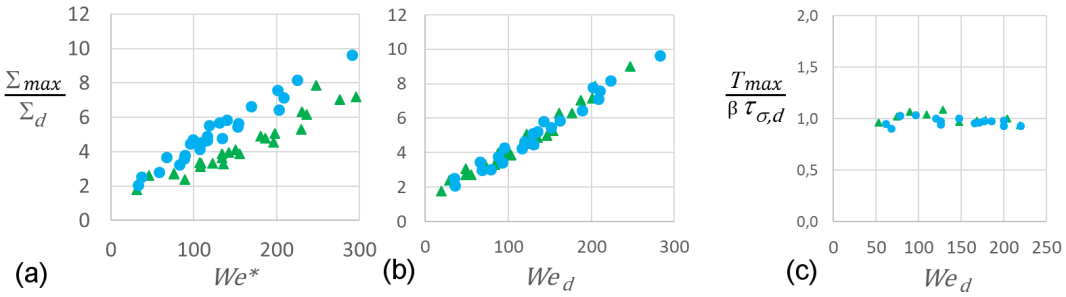

Figure 7. Σ_{max}/Σ_d as a function of (a) We^* and (b) We_d . (c) $T_{max}/\beta\tau_{\sigma,d}$ with β a constant equal to 0.34.

period of the drop ($\propto \tau_{\sigma,d}$), independently from the encapsulating liquid and from the drop velocity. It is noteworthy that using a different capillary time scale, such as $\tau_{\sigma,dj} = \sqrt{m_d/\sigma_{dj}}$ calculated with the interfacial tension, or $\tau_{\sigma,total} = \sqrt{(m_d + m_j)/(\sigma_d + \sigma_j)}$ obtained considering both the drops and the jet, does not enable to bring all normalized T_{max} around the same values (not shown). Thus, for the investigated range of U and similarly to the extent of drop expansion, the kinetics of it seems to be only driven by the drop capillary time. This confirms that We_d could be more appropriate than We^* to describe these collisions. Interestingly, similar kinetics have already been reported for immiscible drop collisions [14], but not for drops impacting onto immiscible liquid films where both liquids must be accounted for [15].
Having shown that, for immiscible liquids, the prediction of D_{max} is better using We_d than We^*, the evaluation of the fragmentation criterion $D_{max}^2 >> D_{dij}L_{dij}$ can still be questioned.
To answer this point, we observe for large L_j/D_j the drop extension at the fragmentation limit. We denote $\zeta = L_{max}/D_d$ the normalized lateral extension of the drop during the recoil phase, see Fig. 8a). As shown in Fig. 8b) and c), ζ follows the same evolution with We_d for both silicon oil and hexadecane. The full symbols corresponding to *drops in jet* and the empty ones to *fragmented drops in jet*, we cannot identify a significant shift in the critical values leading to the drop fragmentation.

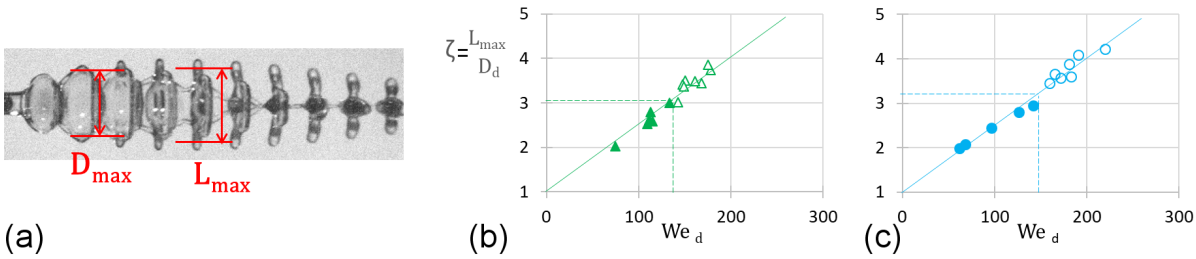

Figure 8. a) definition of $\zeta = L_{max}/D_d$; ζ against We_d obtained for $L_j/D_j > 1.5$ with (b) silicon oil and (c) hexadecane. Full symbols: *drops-in-jet*, empty symbols: *fragmented drops in jet* or *mixed fragmentation*.

To better evaluate this point, the data of Fig. 5 are plotted using (L_j/D_j, $We_d{D_d}^2/D_{dij}L_{dij}$), see Fig. 9. For the two immiscible liquid pairs (a and b), the drop fragmentation limits (transition between *drops-in-jet* and *fragmented drops in jet* for small L_j/D_j and between *encapsulated drops* and *mixed fragmentation* for large L_j/D_j) appear similar, indicating that $D_{dij}L_{dij}$ is a good candidate for a fragmentation criterion of the drop.

For miscible liquids, comparing silicon oil and the ethanol mixture (Fig. 9a) and c)) shows a clear shift in the limit of fragmentation found for large L_j/D_j, which may be due to a surface tension gradient. For lower L_j/D_j, *fragmented drops in jet* seem to be partially replaced by *mixed fragmentation*. Indeed, this is probably a consequence of the liquid miscibility. Due to this miscibility, *fragmented drops in jet* can only be identified if part of the drops are expelled from the continuous jet. This seems not to appear for $L_j/D_j \approx 1.7$. Instead, the drop fragments drag the jet and cause its fragmentation; the jet does not remain continuous anymore. For the ethanol mixture the disappearance of the *drops-in-jet* can indeed only be caused by the deformation of the liquid envelop and not by the drops alone. Further analysis of this process will be presented in a forthcoming paper.

Conclusions

We have shown that the outcomes of drops-jet collisions are influenced by the wettability and miscibility of the liquid pairs. We used three liquid pairs to compare a jet totally wetting the drops (silicon oil and glycerol mixture), a jet partially wetting the drops (hexadecane and glycerol mixture) and a jet miscible with the drops (ethanol mixture and glycerol mixture). If the same kinds of regimes are found for all cases, their occurrence described using the geometric parameter L_j/D_j and the inertial one $We^*{D_d}^2/D_{dij}L_{dij}$ are significantly shifted.
As proposed for silicon oil and regardless of the nature of the jet liquid, a capillary fragmentation of the jet seems to happen when a critical value of L_j/D_j is reached. By comparison to a totally wetting jet, a partially wetting jet

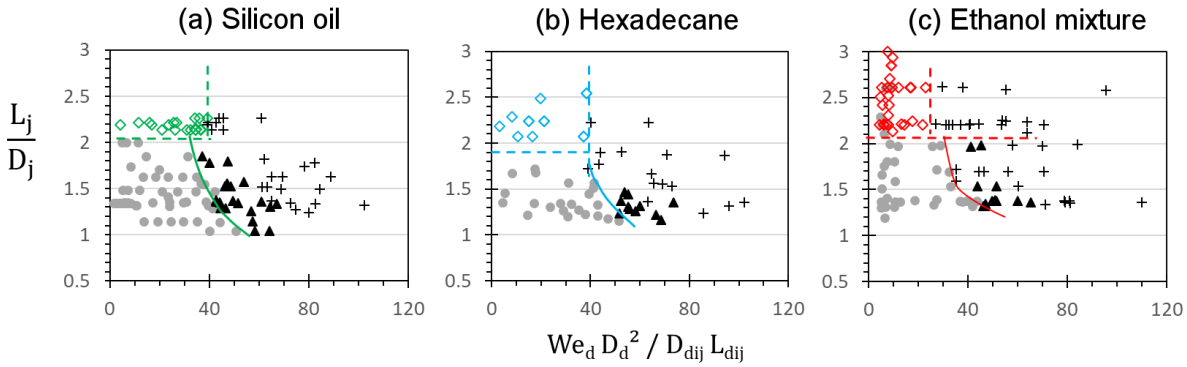

Figure 9. Regime maps using (L_j/D_j; $We_d {D_d}^2/L_{dij}D_{dij}$) obtained with a jet of a) silicon oil; b) hexadecane and c) ethanol-water mixture. Grey circles: *drops in jet*; black triangles: *fragmented drops in jet*; black crosses: *mixed fragmentation*; green and blue diamonds (a-b): *encapsulated drops* and red diamonds (c): *fragmented jet*. The lines are guides for the eye.

seems to slightly decrease the critical value of L_j/D_j, thus destabilizing the capillary fragmentation of the jet. Yet, careful interpretation of this result must be done since the variations remain within the range of typical experimental uncertainty. Possible jet destabilization could be caused by greater Laplace pressure of the encapsulated drops. Comparing the totally wetting jet to the one miscible with the drops does not show significant differences: the capillary limit remains around $L_j/D_j \approx 2$.
The inertial fragmentation limit found for silicon oil for a critical value of $We^* {D_d}^2/D_{dij}L_{dij}$ is also observed for hexadecane and the ethanol mixture. Qualitatively, the transitions are similar in that they go from *encapsulated drops* or *fragmented jet* to *mixed fragmentation* for large L_j/D_j and miscible or immiscible liquids, respectively, and from *drops in jet* to *fragmented drops in jet* and *mixed fragmentation* when L_j/D_j is small for both immiscible and miscible liquids. Yet, the transitions are not found for the same values of $We^* {D_d}^2/D_{dij}L_{dij}$. Since this parameter was built to compare the maximum extension of the drop D_{max} to the typical dimensions of the *drops-in-jet* structure, namely D_{dij} and L_{dij}, but using an unoptimized scaling for D_{max}, this result is not surprising. Correcting the scaling of D_{max} using We_d instead of We^* enables to bring the transitions around the same values of ${D_{max}}^2/D_{dij}L_{dij}$ for small L_j/D_j.
For larger values of L_j/D_j, the miscibility of the liquids considerably reduces the stability of the jet. This may be interpreted as the consequence of periodic surface tension gradients which could destabilize the jet.

Acknowledgements
We would like to acknowledge the FWF (Austrian Science Fund) for its financial support to the project under the Grant number P31064-N36. We would also like to acknowledge the GRK2160/1 “DROPIT" summer school and its organizational team for their financial support. We are indebted to R. Bernard and G. Lamanna for the stimulating discussions and exchanges during the joint summer school project.

Nomenclature

j	subscript for jet or jet liquid
d	subscript for drop or drop liquid
ij	subscript for drop-jet interface
dij	subscript for drop-in-jet regime
ρ	liquid density
σ	surface or interfacial tension
μ	viscosity
We	Weber number
D	diameter
L	spatial period
$\vec{u}$	velocity
$\vec{U}$	relative velocity
$\perp$	subscript for orthogonal to the jet axis
$\parallel$	subscript for tangential to the jet axis

References

[1] Y. Yeo, A. U. Chen, O. A. Basaran, and K. Park, 2004, *Pharm. Res.*, 21, 1419.
[2] H. Hinterbichler, C. Planchette, and G. Brenn , *Exp. Fluids* , 56, 190.
[3] C. Planchette, H. Hinterbichler, and G. Brenn, 2017, *Proceedings of ILASS-Europe*, Spain.

[4] C.W. Visser, T. Kamperman, L. P. Karbaat, D. Lohse, and M. Karperien, 2018, *Sci. Adv.*, 4 (eaaol175).
[5] T. Kamperman,V.D.Trikalitis,M. Karperien,C.W.Visser, and J.Leijten, 2018, *ACS Appl. Mater. Interfaces*, 10, 23433.
[6] R.H. Chen, S.L. Chiu, and T.H. Lin, 2006, *Exp. Therm. Fluid Sci.*, 31, 75.
[7] C. Planchette, S. Petit, H. Hinterbichler, and G. Brenn, 2018, *Phys. Rev. Fluids*, 3, 093603.
[8] C. Planchette, E. Lorenceau, and G. Brenn, 2012, *J. Fluid. Mech*, 702, pp 5-25.
[9] F. Peters and D. Arabali, 2013, *Colloids and Surfaces A*, pp 1-5.
[10] A. Goebel and K. Lunkenheimer, 1997, *Langmuir* , pp. 369-372.
[11] S. Zeppieri, J. Rodriguez and A. L. Lopez de Ramos, 2001, *Journal of Chemical Engineering Data*, pp 1086-1088.
[12] S. Chandra and C. T. Avedisian, 1991, *Proc. R. Soc. A*, 432, 13.
[13] K. D. Willis, and M. Orme, 2003, *Exp. Fluids*, 34, pp 28–41.
[14] C. Planchette, H. Hinterbichler, M. Liu, D. Bothe and G. Brenn, 2017, *J. Fluid. Mech*, 814, pp 277-300.
[15] R. Bernard and G. Lammana, University of Stuttgart, 2018, DROPIT summer School, Germany, private communications.